

Code assessment and modelling for Design Basis Accident Analysis of the European sodium fast reactor design. Part I: System description, modelling and benchmarking

A. Lázaro^{a,i,*}, L. Ammirabile^a, G. Bandini^b, G. Darmet^c, S. Massara^{c,1}, Ph. Dufour^d, A. Tosello^d, E. Gallego^e, G. Jimenez^e, K. Mikityuk^f, M. Schikorr^g, E. Bubelis^g, A. Ponomarev^g, R. Kruessmann^g, M. Stempniewicz^h

^a JRC-IET European Commission—Westerduinweg 3, PO Box-2, 1755 ZG Petten, The Netherlands

^b ENEA, Via Martiri di Monte Sole 4, 40129 Bologna, Italy

^c EDF, 1 avenue du Général de Gaulle, 92141 Clamart, France

^d CEA, St Paul lez Durance, 13108 Cadarache, France

^e UPM, José Gutiérrez Abascal, 2-28006 Madrid, Spain

^f PSI—Paul Scherrer Institut, 5232 Villigen Switzerland

^g KIT—Institute for Neutron Physics and Reactor Technology, Hermann-von-Helmholtz-Platz 1, 76344 Eggenstein-Leopoldshafen Germany

^h NRG, Utrechtseweg 310, PO Box 9034 6800 ES, Arnhem, The Netherlands

ⁱ UPV—Universidad Politécnica de Valencia, Camí de vera s/n-46002, Valencia, Spain



HIGHLIGHTS

- Ten system-code models of the ESFR were developed in the frame of the CP-ESFR project.
- Eight different thermohydraulic system codes adapted to sodium fast reactor's technology.
- Benchmarking exercise settled to check the consistency of the calculations.
- Upgraded system codes able to simulate the reactivity feedback and key safety parameters.

ARTICLE INFO

Article history:

Received 29 April 2013

Received in revised form 11 October 2013

Accepted 16 October 2013

ABSTRACT

The new reactor concepts proposed in the Generation IV International Forum (GIF) are conceived to improve the use of natural resources, reduce the amount of high-level radioactive waste and excel in their reliability and safe operation. Among these novel designs sodium fast reactors (SFRs) stand out due to their technological feasibility as demonstrated in several countries during the last decades. As part of the contribution of EURATOM to GIF the CP-ESFR is a collaborative project with the objective, among others, to perform extensive analysis on safety issues involving renewed SFR demonstrator designs. The verification of computational tools able to simulate the plant behaviour under postulated accidental conditions by code-to-code comparison was identified as a key point to ensure reactor safety. In this line, several organizations employed coupled neutronic and thermal-hydraulic system codes able to simulate complex and specific phenomena involving multi-physics studies adapted to this particular fast reactor technology. In the "Introduction" of this paper the framework of this study is discussed, the second section describes the envisaged plant design and the commonly agreed upon modelling guidelines. The third section presents a comparative analysis of the calculations performed by each organisation applying their models and codes to a common agreed transient with the objective to harmonize the models as well as validating the implementation of all relevant physical phenomena in the different system codes.

© 2013 Elsevier B.V. All rights reserved.

1. Introduction

Fast reactors are identified in the Generation IV International Forum Roadmap (GIF; [Gen and Roadmap, 2002](#)) as a unique, potentially sustainable energy source in terms of waste management, fuel optimisation, economic competitiveness and proliferation

* Corresponding author. Tel.: +31 224 56 5446.

E-mail address: aurelio.lazaro-chueca@ec.europa.eu (A. Lázaro).

¹ OECD-NEA 12, boulevard des îles 92130, Issy-les-Moulineaux, France.

resistance. Among the proposed designs, Sodium fast reactors (SFR) have the advantage of the extensive technological experience gained during past and current projects as developed in many different countries for nearly 50 years. In particular, the design and operation of several prototypical sodium-cooled fast reactors, such as the Experimental Breeder Reactor (EBR) and the Fast Flux Test Facility (FFTF) in Hanford (USA), the prototype Phénix in France (Sauvage, 2005), the BN-350 in Kazakhstan, and Monju in Japan (Matsuura et al., 2007; Kondo et al., 2013) have accumulated a total of about 400 reactor-years of operational experience in SFR technology. Currently, the sodium-cooled China Experimental Fast Reactor (CEFR) (Xu, 2000) has been connected to the grid in July 2011, while the Russian BN-800 (Saraev et al., 2012) and the Prototype Fast Breeder Reactor (PFBR) in India (Chetal et al., 2006) are both under construction. In Europe the advanced sodium technological reactor for industrial demonstration ASTRID (Le Coz, 2013) is planned as demonstration project within the “European Sustainable Nuclear Industrial Initiative” (ESNII, 2009; European Utility Requirements, 2001). Several European countries are currently active in research programmes for the development of fast reactors innovative (GENIV) concepts.

In order to create a common European framework to support the sodium fast reactor technology and as part of the EURATOM contribution to the GIF, the Collaborative Project on the European Sodium Fast Reactor (CP-ESFR) was conducted within the 7th EURATOM Framework programme (Vasile et al., 2011).

The project merged the contribution of 24 European partners with the objective to establish the technical basis of a European sodium fast reactor plant with enhanced safety performance, resource efficiency and cost-effectiveness.

The project was divided into several work packages (Vasile et al., 2011) covering the different technical aspects of the reactor design. In particular the work package number three (WP3) focused on the safety assessment of the plant and its subsystems. Its main objectives were the definition of an adequate safety approach with safety objectives and principles for the design; the proposal of preliminary assessment of provisions related to the implementation of the whole set of defence in depth levels; studies of representative transients; and scenarios and the evaluation of design strategies to limit the consequences of a partial core disruptive situation.

Innovative nuclear reactor design concepts require specific tools to assess reactor performance and safety. Compared to the traditional water-cooled thermal nuclear reactors the use of sodium as coolant, the fast neutron kinetics, and the pool-type design are some of the design options that call for the development and validation of computational tools able to analyse the safety features of these innovative systems that may affect the global plant safety. A specific task (Task 3.3.1) was established with the objective to develop multi-physics models for the plant design and perform calculations to evaluate the behaviour of the plant during certain postulated transients.

The task group consisted of eight organisations namely, CEA (France), ENEA (Italy), EDF (France), UPM (Spain), PSI (Switzerland), KIT (Germany), NRG (Netherlands) and JRC-IET (European Commission). Each organisation provided its expertise on the use of dedicated system codes adapted for sodium-cooled fast reactor applications. Some computational tools, originally developed for commercial light water nuclear reactor safety analyses, have undergone extensive modifications (coolant material properties, heat transfer correlations and pressure drop models) to be applied for SFR studies.

The approach followed was to set up a benchmarking exercise. First, each organisation amended the modelling of their employed system codes according to the ESFR plant specifics (primary, secondary, tertiary loops). Calculated results of a defined transient were then compared with those of the other partners allowing collective modelling iteration and enhancements in the various codes. In this respect, this benchmark exercise provided the unique opportunity to compare the performance of the current state-of-the-art system codes for applications related to sodium-cooled fast reactor safety analyses. In Section 2 we present the reference European sodium fast reactor design (Ehster, 2009) adopted in the safety studies: an oxide-fuelled, pool-type reactor. The system codes used in the task are shortly described in Section 3 while some common modeling aspects are given in Section 4. In Section 5 we present the main results of the comparison case. Specific aspects and phenomena that required refinement in the modeling in order to achieve higher accuracy in the results are identified, and the main conclusions of the study are outlined. Discussion and conclusions are presented in Section 6.

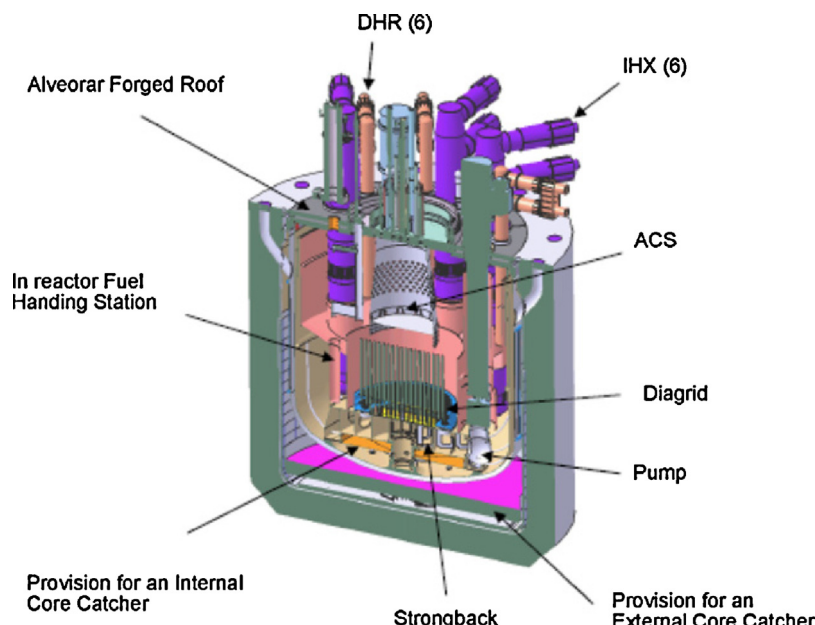


Fig. 1. ESFR pool-type concept (Vasile et al., 2011).

2. The European sodium fast reactor design

The plant design (Genot, 2009; Blanchet and Buiron, 2009) is based on an industrial sodium cooled pool reactor of 1500 MWe. The reactor has three coolant systems: a primary sodium coolant system, an intermediate sodium coolant system, and a steam-water, turbine-condenser coolant system. The pool-type primary system includes the core, three mechanical primary pumps (PP) and six Intermediate Heat Exchangers (IHX) (Fig. 1). Six Decay Heat Removal systems (DHR) connected to six Direct Reactor Cooling loops (DRC) are also present to ensure decay heat removal of the reactor upon shut down. The coolant flows upward through the reactor core into the upper sodium pool (plenum) of the main vessel. From the upper plenum the sodium flows downward through the intermediate heat exchanger and discharges into a lower sodium pool. The vertically oriented primary pumps draw the coolant from the lower pool and discharge it into the core inlet plenum. The secondary system consists of six intermediate loops, each equipped with one Intermediate Heat Exchanger (IHX) on the reactor side and six modular sodium/water Steam Generators (SG) of 100 MW_{th} power capacity each.

The tertiary system consists therefore of 36 separate circuits. The high temperature steam is used to drive a conventional turbine to produce electricity.

The SFR oxide core layout consists of an inner and outer fuel region with different Pu mass content in order to flatten the radial core power profile at end of cycle. There are 225 inner fuel sub-assemblies and 228 outer fuel sub-assemblies. The control rod system is composed of 9 DSD (Diverse Shutdown Device) and 24 CSD (Control and Shutdown Device). The CSD rod absorber contains natural boron carbide whereas the DSD rod absorber contains enriched boron carbide. The reflectors consist of three rings of assemblies with two additional rows of dedicated assemblies or alternative devices such as steel blocks for shielding.

The fuel sub-assembly consists of a hexagonal wrapper tube that contains a triangular arrangement of 271 fuel pins with helical wire wrap spacers. The fuel pin consists of (U,Pu)O₂ pellets in ODS steel cladding. The fissile zone is 1 m high. The lower blanket is filled with steel pellets.

In general terms the ESFR core is flat ("pancake" design) to provide good thermal-hydraulic properties and to enhance neutron leakage in order to reduce the sodium void effect. The breeding gain is about 1.04. The main reactor parameters are summarized in Table 1.

The core radial layout is shown in Fig. 2 and the core axial layout is shown in Fig. 3.

The main thermodynamic variables in nominal conditions are listed in Table 1.

3. Codes

The system codes used by the different organisations are the following:

- ENEA RELAP5 and CATHARE
- PSI TRACE-FRED
- JRC/UPV RELAP5 and TRACE
- KIT SIM-SFR, SAS-SFR
- EdF MAT4-DYN
- CEA CATHARE
- NRG SPECTRA

The TRACE (TRAC-RELAP Advanced Computational Engine) code is the latest in a series of best-estimate system codes developed by the U.S. Nuclear Regulatory Commission for analysing

Table 1
Nominal conditions and plant parameters of the ESFR pool-type plant.

Variable	
Reactor power (MW _{th})	3600
Number of FA	453
Number of pins per FA	271
Fuel pin outer clad diameter (mm)	10.73
Fuel pin inner clad diameter (mm)	9.73
Fuel pellet outer diameter (mm)	9.43
Fuel pellet inner diameter (mm)	2.4
Cladding material	ODS Steel
Fuel pellet material	(U,Pu)O ₂
Average burn-up (GWD/tHM)	100
Core average plutonium factor (%)	15.7
Core inlet temperature (°C)	395
Core outlet temperature (°C)	545
Average core structure temperature (°C)	470
Average fuel temperature (°C)	1227
Total primary mass flow rate (kg/s)	19535
Primary Na inventory (m ³)	2612.8
Total secondary massflow rate (kg/s)	15,330
Secondary coolant temperature at IHX inlet (°C)	525
Secondary coolant temperature at IHX outlet (°C)	340
Water temperature at SG inlet (°C)	240
Water temperature at SG outlet (°C)	490
Steam pressure (MPa)	18.5

steady-state and transient thermohydraulic-neutronic behaviour in light water reactors (NRC, 2007). Models used include multi-dimensional two-phase flow, non-equilibrium thermodynamics, generalized heat transfer, reflooding, level tracking and neutron kinetics. The officially-released version doesn't support biphasic liquid metal flows but adaptations and modifications made by various European organizations, in particular PSI, allow this code now to be applied also for SFR analysis under sodium boiling conditions (Chenu, 2011a,b). The FRED code (Mikityuk and Shestopalov, 2011) coupled to TRACE was used at PSI to simulate the evolution of thermal and stress-strain conditions in fuel rods.

The RELAP5 (RELAP, 1995) code used for the transient analysis of the ESFR reactor is a modified version of the RELAP5/MOD3.3 code,

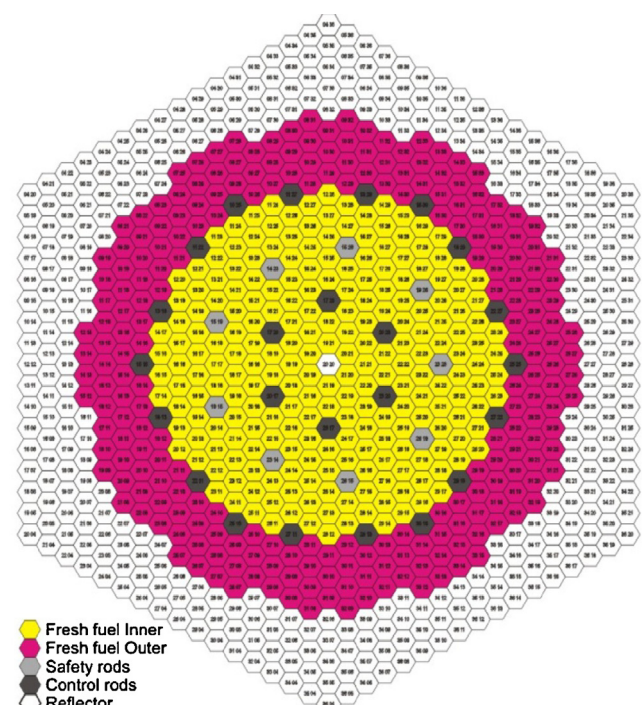


Fig. 2. Oxide core radial layout (Vasile et al., 2011).

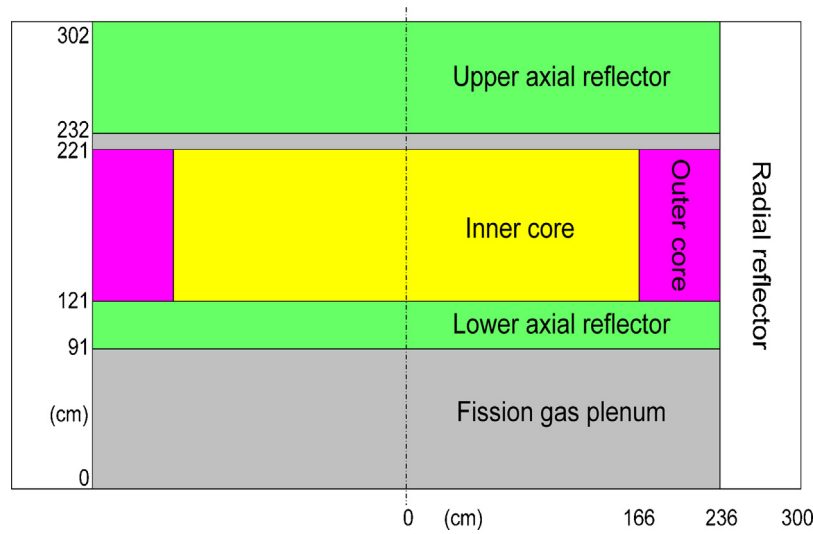


Fig. 3. Axial configuration of the reference core (Genot, 2009; Blanchet and Buiron, 2009).

developed by INEL for the U.S. NRC, currently used world-wide for thermal-hydraulic transient analysis in light water reactors. The features and properties of sodium available in the ATHENA code have been implemented in the modified RELAP5 code. The basic properties for sodium are calculated from optional thermodynamic tables that tabulate saturation and single-phase properties as a function of pressure and temperatures. These tables are based on Young's soft sphere model formulation. Furthermore, the sodium transport properties (viscosity, thermal conductivity and surface tension) from ATHENA have been implemented in the code.

SIM-SFR (Schikorr, 2001) is a system code for the transient analysis of critical and sub-critical reactor concepts developed at KIT during the last two decades. Several reactor concept dedicated versions (SFR, GFR, LFR, HTR, Molten Salt, LWR, and BWR) of the SIM family of codes are available, based on a neutronic multi-nodal (1 to 2-D), fully coupled thermal-hydraulic characterisation of all relevant reactor core internals (fuel pins) as well as the bona-fide modelisation of all the various components of primary, secondary, and tertiary (partially) loops. The core multi-nodal neutronic dynamics is represented by 6 to 8 delayed neutron groups, 13 decay heat groups, along with all the various reactor concept specific reactivity feedback coefficients. The various SIM code versions have been validated against actual reactor plant transients and other major transient code systems (RELAP, CATHARE, TRACE, etc., see above and below) and used extensively throughout various European projects (PDS-XADS, MOST, LEADER, EUROTRANS, GFR, GoFastR, CP-ESFR, EVOL, etc.) during the last decade.

MAT4-DYN (Massara et al., 2005) is based on a very simplified thermo-hydraulic model coupled with a point-kinetic solver fed with six groups delayed neutrons. MAT4-DYN is limited to a single channel description. Sodium is single-phase. Particularly, that benchmark has allowed EDF to point out strong similarities between MAT4-DYN code and the ones developed (or used) by the other participants. Indeed, and by comparison to other codes, we see in the following paragraphs that MAT4-DYN relies on two strong hypothesis that have a non-negligible impact on results:

- a mono-channel description, that introduce a physical bias between the real core and the simulated one and significantly impact the Doppler feedback reactivity during the short time transient,
- a simplified IHX model that impact the inlet core temperature during the mid-term transient.

These weaknesses of the MAT4-DYN code have led EDF to develop a multi-channel code named MAT5-DYN (Darmet and Massara, 2012).

SPECTRA (Sophisticated Plant Evaluation Code for Thermal-hydraulic Response Assessment) (NRG, 2010) is a system code developed at NRG. The code is designed for transient thermal-hydraulic and neutronic analyses of nuclear power plants. Models include two-phase flows, non-equilibrium thermodynamics, 1-D and 2-D conduction, thermal radiation, point reactor kinetics including isotope chains and feedback from isotopes (Xe-135, etc.). The code is applicable and validated for LWR, HTR/PBMR, GCFR, LMFR. In the case of liquid metal reactors the thermodynamic and thermophysical properties of coolant, as well as heat transfer correlations are supplied by the user.

CATHARE 2 code (Geffraye et al., 2011) is the outcome of more than 30 years of joint development effort by CEA (French Atomic Energy Commission), EdF (Electricité de France), AREVA-NP and IRSN (Radio-protection and Nuclear Safety Institute). CATHARE 2 was originally conceived for safety studies of PWR systems, recently extended in the framework of the Generation IV International Forum to other nuclear reactors, particularly to Sodium-cooled Fast Reactors (SFR). The know-how of codes formerly used for Superphenix (SPX) reactor transients computation has been retrieved. These developments have been validated by comparison with other codes and experimental results. CATHARE 2 has now been used for the study of innovative SFR designs since 2008. CATHARE 2 has a flexible modular structure for the thermal-hydraulic modeling in applications ranging from simple experimental test facilities to large and complex installations like Nuclear Power Plants. The discretization of all terms of the equations is fully implicit in 1D and 0D modules and semi-implicit in 3D elements including inter-phase exchange, pressure and convection terms, and the resulting non-linear equations are solved using an iterative Newton solver. The code allows efficient use of several processors in parallel.

SAS-SFR (Safety Analyses System code for Sodium-cooled Fast Reactors) was developed by ANL since the 1960s and continuously improved by a consortium formed by KIT, CEA, IRSN, and JAEA. Its purpose is the analysis of the behaviour of liquid-metal cooled, in particular sodium-cooled fast reactors in design-basis, and particularly in beyond-design-basis accidents. To perform transient analyses with SAS-SFR, the SFR core geometry is normally subdivided into many (10 in the case of ESFR) different axial flow/power channels and the plant characteristics are also represented appropriately. In addition specific subassembly (SA) design

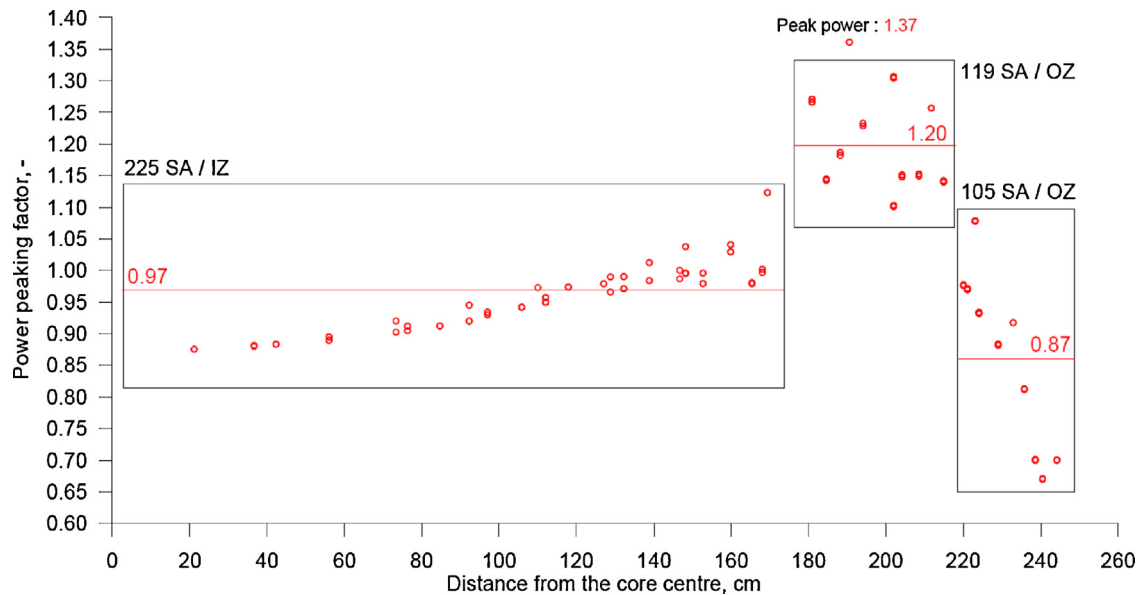


Fig. 4. Fuel assembly-wise power distribution at BOL (Mikityuk and Krepel, 2010).

characteristics are taken into consideration for the appropriate evaluation of the transient thermal-hydraulic and fuel pin mechanics behaviour under different core burn-up conditions (BOL, EOL, etc.).

4. Modelling

The ESFR technical design was translated into code-specific input data sets to simulate the system behaviour. Each code user was responsible to choose appropriate inputs and models able to represent the behaviour of the various plant subsystems. This process required to some extend code adaptations and in some cases simplifications and assumptions that could affect the final results.

One of the added values of the benchmarking exercise performed was to harmonize these criteria and to reach a common agreement in modelling assumptions. Nevertheless, some remaining differences can be attributed to the so-called user effect.

4.1. Core model

Based on the analysis of the power distribution at the Beginning of Life (BOL), see Fig. 4, a core model consisting of several parallel channels was proposed to be used in the transient calculations (7 in case of TRACE/FRED, see Fig. 5). The seven simulated regions correspond to:

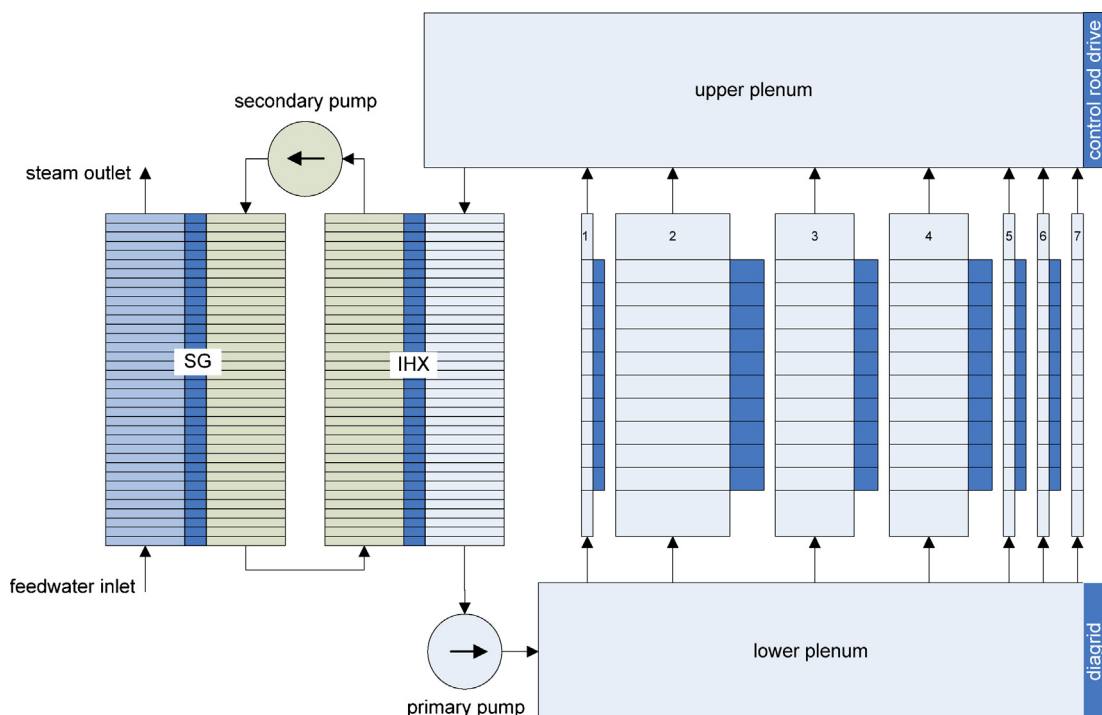


Fig. 5. Proposed thermohydraulic core model (Mikityuk and Krepel, 2010) and simplified plant model.

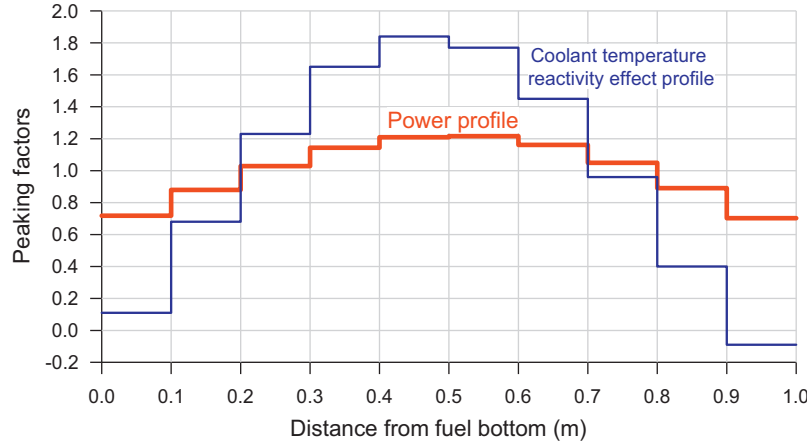


Fig. 6. Axial profiles of power and coolant temperature reactivity effect.

- One channel for the hot fuel assembly. (1)
- One channel for the whole inner zone representing 225 fuel sub-assemblies. (2)
- Two channels representing the core outer zones, with 119 and 105 fuel subassemblies respectively (3 and 4).
- One channel for the central dummy and control assemblies (5).
- One channel for the reflector (6).
- One channel for the inter-assemblies by-pass (7).

The axial power distribution used in the analysis is shown in Fig. 6.

4.2. Point kinetics model

Since most of the system codes used by the different partners are only able to simulate the neutronic response of the system using a point kinetics model, the reactivity coefficients and other kinetics parameters were specified as input in addition to the radial and axial power distribution described in the previous section. The use of point kinetics model limits the neutronic analyses to radially core-symmetric transient scenarios while core-asymmetrical transients require necessarily the coupling with 3D neutron kinetics codes.

The neutronic response has been modelled considering the following six reactivity effects as proposed in (Mikityuk and Krepel, 2010):

1. *Doppler effect*: This effect has been calculated using the following expression:

$$\Delta\rho_D = K_D \cdot \ln(T_{fuel}/T_{fuel0}) \quad (1)$$

where K_D is the Doppler constant and T_{fuel} and T_{fuel0} are the transient and nominal core-average fuel temperatures (K) respectively.

2. *Coolant temperature effect*: this effect has been calculated using the following expression:

$$\Delta\rho_{cool} = \sum_i \chi^i \cdot c_T \cdot (T_{cool}^i - T_{cool0}^i) \quad (2)$$

where c_T is the coolant temperature reactivity coefficient χ^i is the axial contribution of the node, such that $\sum_i \chi^i = 1$ and T_{cool} and T_{cool0} are the transient and nominal coolant temperatures in the node. The axial profile of the coolant temperature reactivity effect is shown in Fig. 6, due to the leakage component of the

effect, the profile steeply reduces towards the axial reflector and even becomes negative close to the upper reflector.

3. *Fuel expansion effect*: The increase of the core average fuel column height will reduce the total reactivity due to the reduction of the in-core fuel density and the increase of the neutron leakage. The fuel column was assumed to be not bonded by the cladding and expanding freely driven by the average fuel temperature. This effect has been modelled as follows:

$$\Delta\rho_{f,\exp} = c_{f,\exp} (T_{fuel} - T_{fuel0}) \quad (3)$$

where $c_{f,\exp}$ is the fuel expansion reactivity coefficient [pcm/K], while T_{fuel} and T_{fuel0} are the transient and nominal core-averaged fuel temperatures.

4. *Cladding expansion effect*: The axial expansion of the cladding will cause an increase in the total reactivity due to the reduction of the in-core parasitic absorption by the stainless steel and a reduction of the sodium volume fraction due to the radial expansion of the cladding. This effect has been modelled as follows:

$$\Delta\rho_{c,\exp} = c_{c,\exp} \cdot (T_{clad} - T_{clad0}) \quad (4)$$

where $c_{c,\exp}$ is the cladding expansion reactivity coefficient [pcm/K], while T_{clad} and T_{clad0} are the transient and nominal core-average clad temperatures.

5. *Diagrid expansion effect*: The diagrid thermal expansion effect will increase the radius of the core reducing the in-core smeared fuel density and increasing the neutronic leakage from the core. This effect has been modelled using the expression that follows,

$$\Delta\rho_{diagrid} = c_{diagrid} \cdot (T_{diag} - T_{diag0}) \quad (5)$$

where $c_{diagrid}$ is the diagrid expansion reactivity coefficient [pcm/K] and T_{diag} and T_{diag0} are the transient and nominal diagrid temperatures.

6. *Differential core/control rods expansion effect*: During a loss of flow transient in a fast reactor, one of the most important feedbacks is due to the relative axial displacement of the core and control rods. A simplified simulation of the reactivity feedback caused by a thermal expansion of the control rod driveline (CRD) mechanisms combined with the thermal expansion of the core support structures (CSS) was recommended by CEA for the benchmark, based on the operational experience of SPX1.

The axial insertion of the control rods Δz_1 due to the CRD thermal expansion corresponding to the CRD temperature increase ΔT_1 given by $\Delta z_1 = \alpha_1 \Delta T_1$, where α_1 is the thermal expansion coefficient of the CRD material (the recommended value is 0.15 mm/°C).

Table 2
Point kinetic reactivity coefficients.

Reactivity Coefficients	
Doppler constant KD (pcm)	-1191
Coolant expansion CT (pcm/K) (Inner/Outer I/Outer II)	0.4/0.1/0.05
Fuel expansion (pcm/K)	-0.1754
Cladding expansion (pcm/K)	0.1485
Diagrid expansion (pcm/K)	-0.5515

The axial upward shift of the core Δz_1 due to the axial thermal expansion of the CSS corresponding to the CSS temperature increase ΔT_2 resulting in the control rods insertion is given by $\Delta z_2 = \alpha_2 \Delta T_2$, where α_2 is the CSS thermal expansion coefficient (the recommended value is 0.11 mm/ $^{\circ}$ C).

The resulting reactivity effect is $\Delta\rho = K(\Delta z_1 + \Delta z_2)$, where K is the corresponding reactivity coefficient (the recommended value is -8.5 pcm/mm).

It was up to the participants to simulate the heat exchange between the core inlet coolant and the CSS as well as between the core outlet coolant and the control rod drive-lines. The CEA recommendation was to assume a small time delay for the CSS temperature response and the time delay parameter for the CRS as follows:

$$\frac{(hA)_1}{(\rho c_p V)_1} = 0.02 \text{ s}^{-1}$$

where $(hA)_1$ is the heat exchange coefficient ($\text{W}/\text{m}^2 \text{C}$) between the core outlet coolant and the CRD times the heat exchange area (m^2), while $(\rho c_p V)_1$ is the volumetric specific heat of the CRD material ($\text{J}/\text{m}^3 \text{C}$) times the CRD volume (m^3).

For the SAS-SFR model, the built-in model was applied with the input values adjusted to what was specified by the project in the framework of the comparison case exercise. In SIM-SFR, a specifically developed control-rod drive-line model was used and appropriately modified, originally benchmarked to several different SPX1 transient data sets, thereby essentially retracing the results of CEA recommended model above under ULOF conditions.

The different values for the reactivity coefficients are shown in Table 2.

In SAS-SFR the reactivity coefficient procedure as proposed above by the project were not used. Instead, the SAS-SFR core model followed an independent, parallel procedure. The values for the

radial and axial material reactivity worth distributions for sodium, fuel, steel and for the Doppler effect coefficients were calculated under BOL core conditions with the modular neutronic code system KANEXT (Becker et al., 2010) on basis of the JEFF 3.1.1 cross section data library. For the chosen 10 channel group allocation there are 8 different reactivity feedback sets considered in accord with the ring wise approach. The sum of all partial feedback values for the Doppler constant and sodium void worth shows good agreement with integral values as calculated by other participants using the project recommended procedure. During the transient, SAS-SFR calculates the cumulated reactivity feedback effects on basis of material reactivity worth distributions and then uses these results within the point kinetics solution algorithm.

4.3. The plant

The primary, intermediate and tertiary systems were modelled by each participant following the technical specifications of the plant provided by other tasks of the ESFR project (Genot, 2009).

Fruitful discussions among the partners helped to solve several uncertainties and simulation challenges closing some gaps in data. Nevertheless, some issues remained unresolved in particular the precise technical specifications of the intermediate system and tertiary systems. The effect of these uncertainties can be observed in some of the results.

The symmetric aspect of the benchmark exercise allowed the simplification of some systems with different loops, IHXs and SGs being lumped together into one or few equivalent nodalizations.

In SAS-SFR, only the primary sodium system was simulated. The secondary IHX sodium temperature field calculated by SIM-SFR (Bubelis and Schikorr, 2012) was used as thermal boundary conditions for the calculation.

A detailed description of each model can be found in the dedicated deliverable generated by the task members (Dufour et al., 2011).

4.4. Models proposed to be used by all participants

The heat transfer coefficient affects the heat transfer capability of all in-vessel and core structures (cladding, wrapper, control rods, sub-assembly, etc.) as well as all heat exchangers (intermediate HX and steam generators). Liquid metals have a much lower Prandtl

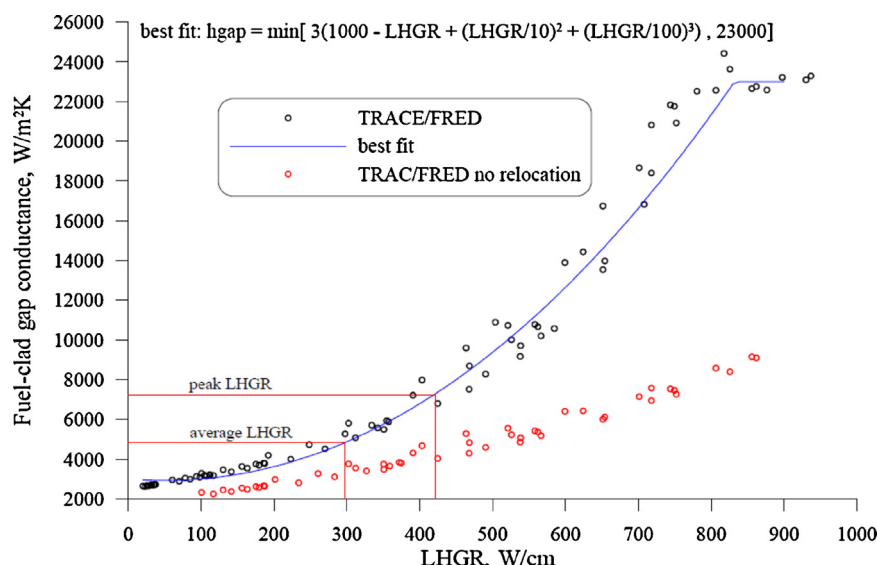


Fig. 7. Results of the parametric study of the fuel-clad gap conductance as a function of the local linear heat generation rate with and without account of fuel relocation, using the TRACE/FRED code.

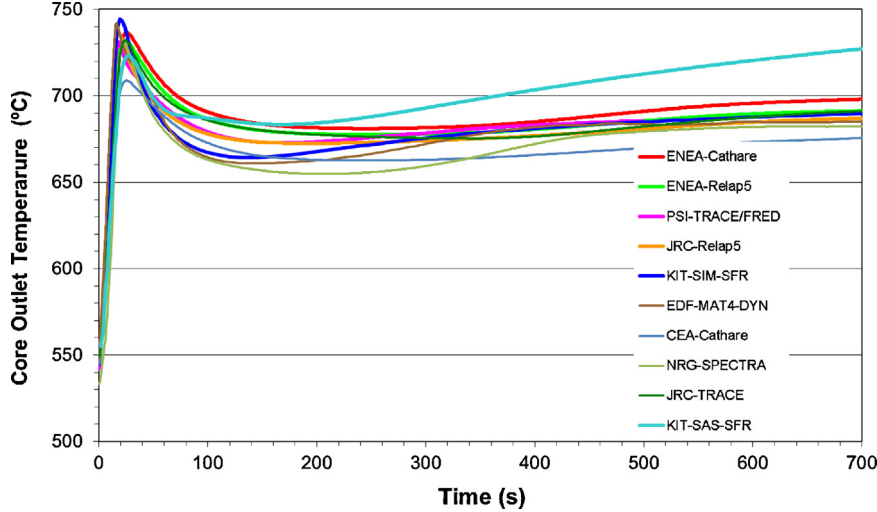


Fig. 8. Core outlet temperature.

number than water, which means that the ratio between the heat transfer due to thermal conductivity and due to convection is much higher for liquid metal. The correlations to take into account this effect differ substantially from the built-in code water correlations, so their replacement become a prerequisite.

In order to harmonize the modelling of this thermal effect, the following correlations were proposed for all participants to be used in the benchmark.

A modification of the Ushakov's correlation ([Mikityuk, 2009](#)) was proposed for simulation of the heat transfer to the developed sodium flow in tube bundles:

$$Nu = 7.55x - \frac{20}{x^{13}} + \frac{0.041}{x^2} Pe^{0.56+0.19x} \quad (6)$$

where Nu is the Nusselt number, x is the pitch-to-diameter ratio and Pe is the Peclet number. This equation can be applied for x from 1.3 to 2.0 and Pe up to 4000.

The Philipponneau correlation ([Philipponneau, 1992](#)) was proposed to be used for calculation of the MOX fuel thermal

conductivity:

$$\lambda = \left(\frac{1}{1.320\sqrt{x} + 0.0093 - 0.091 + 0.038B + 2.493 \cdot 10^{-4}T + 88.4 \times 10^{-12}T^2} \right) \cdot \frac{1-P}{1+2P} \quad (7)$$

where λ is the thermal conductivity (W/m K), x is the deviation from the stoichiometry, B is fuel burnup (at%), T is the fuel temperature (K), P is the fractional porosity.

A parametric study was performed using the TRACE/FRED code in order to derive for the ESFR project ([Fiorini, in press](#)) a dependence of the fuel-clad gap conductance on the local linear heat generation rate. The following correlation was derived and recommended for all participants ([Fig. 7](#)):

$$hgap = \min(3(1000 - LHGR + (\frac{LHGR}{10})^2 + (\frac{LHGR}{100})^3), 23000) \quad (8)$$

where $hgap$ is the gas gap heat conductance (W/m² K) and $LHGR$ the local linear heat generation rate (W/cm). The $hgap$ value is limited

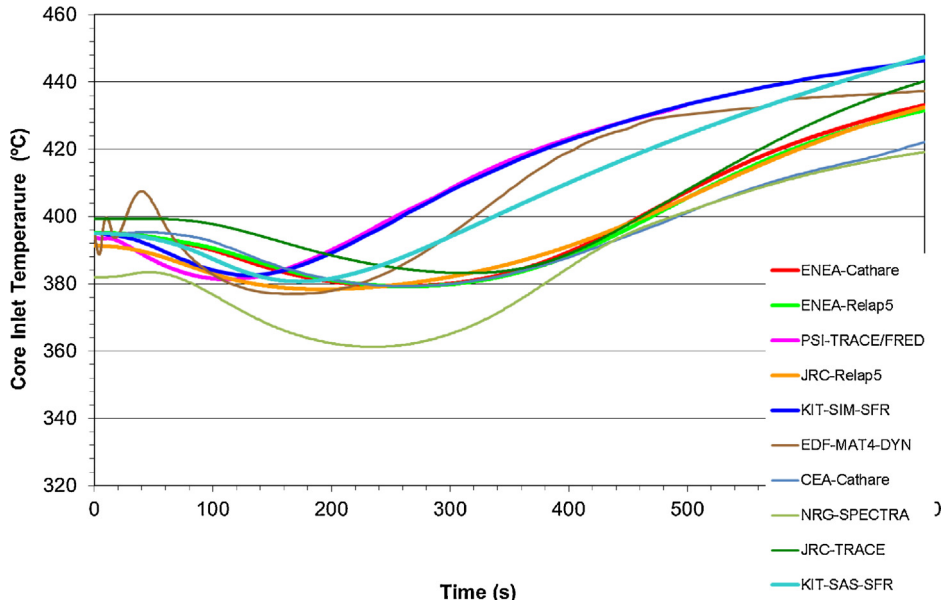


Fig. 9. Core inlet temperature.

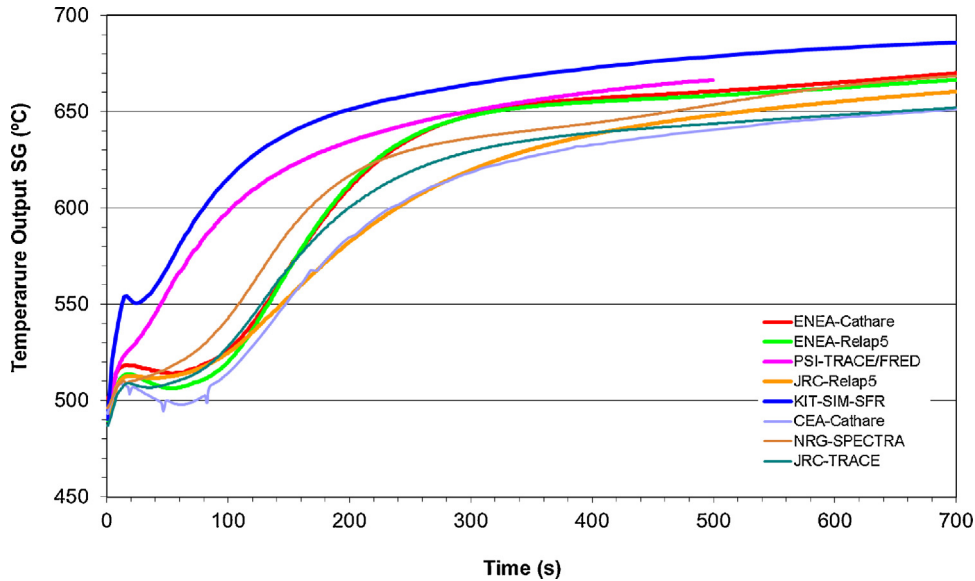


Fig. 10. Steam generator outlet temperature (steam).

from above by $23,000 \text{ W/m}^2 \text{ K}$, corresponding to the closure of the gap.

Instead of this fuel-clad heat conductance dependency on the linear rating, a model already integrated in SAS-SFR which is based on URGAP (Lassmann and Hohlefeld, 1987) was used to calculate the gap heat conductance. SIM-SFR also used its own dynamic fuel gap model (burn-up dependence of both fuel and cladding material), benchmarked to both the SAS-SFR and GERMINAL codes.

Specific pressure drop correlations (Chenu, 2011a,b) may have an impact on the calculation, especially in those transients where natural circulation processes are important. Nevertheless, they were not implemented by all the partners as no natural convection transients were assessed or benchmarked within this current project, but these effects are to be considered in further developments.

5. The comparison case

A somewhat artificial transient was defined by the participants to compare the calculational results attained by the various organisations using different system codes and models. This comparison exercise was recommended to harmonize the different calculational approaches employed in the different code systems.

This transient was defined as a “limited unprotected flow coast-down” event (ULOF), which is characterized by the following simultaneous perturbations:

- The reduction in the primary mass flow-rate to 40% nominal following the equation:

$$Q/Q_0 = \frac{1}{1 + t/10} \quad (9)$$

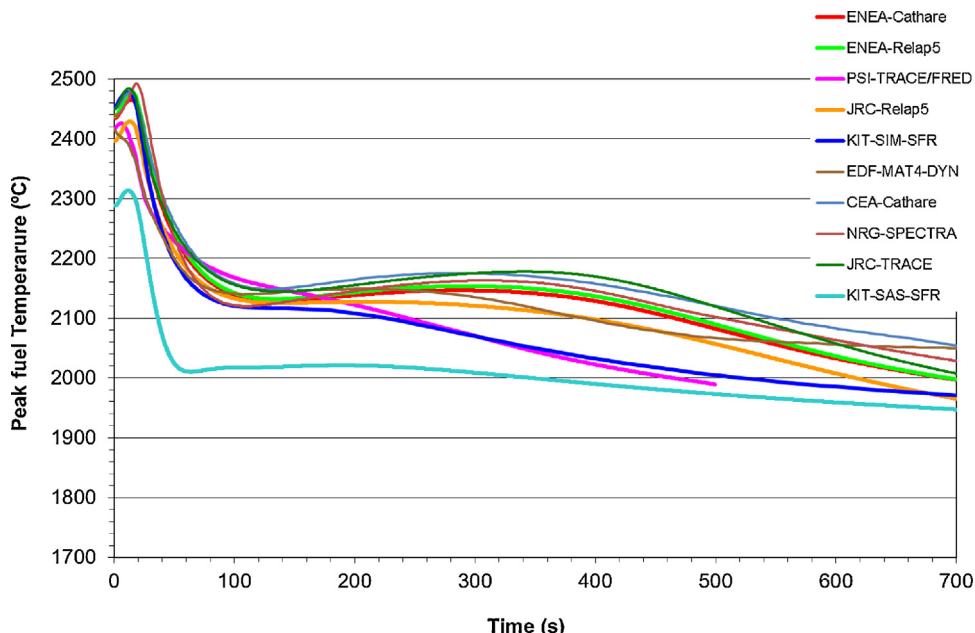


Fig. 11. Peak fuel temperature.

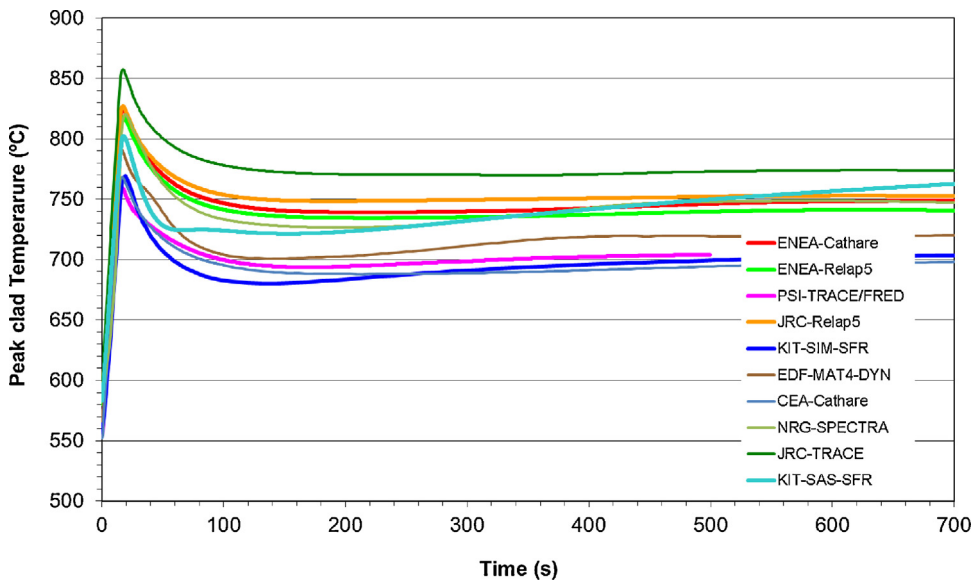


Fig. 12. Peak cladding temperature.

- The reduction in the secondary mass flow-rate to 40% nominal following the equation :

$$Q/Q_0 = 1 - 0.094t \quad (10)$$

- Reduction of the feedwater mass flow-rate in the water side of the steam generators, decreasing from its nominal value to 50% in 6 s.

- The reactor is unprotected (does not trip).

The mass flow-rates (primary, secondary, tertiary) were assumed to remain constant after reaching their asymptotic states. Figs. 8–21 show the time evolution of the main safety related variables of the ESFR plant during the first 700 s of the limited ULOF transient. These variables are namely,

- Core inlet and outlet temperatures.
- Steam generator outlet steam temperature.

- Peak fuel and cladding temperatures.
- Total reactivity and its different components (Doppler, coolant temperature, fuel and cladding expansion, diagrid expansion and differential core/control rods expansion).
- Reactor, intermediate heat exchanger and steam generators powers.

5.1. Coolant temperatures

Fig. 8 shows the temperature evolution of the sodium coolant at the hot fuel assembly outlet and in Fig. 9 the evolution of the core inlet temperature is displayed. The abrupt increase in outlet temperature as a consequence of the massflow reduction triggering the transient can be observed. All the calculations performed by the different partners predict quite similar coolant maximum outlet temperatures taking into account that most of the codes use somewhat different sodium specific heat correlations and core inlet

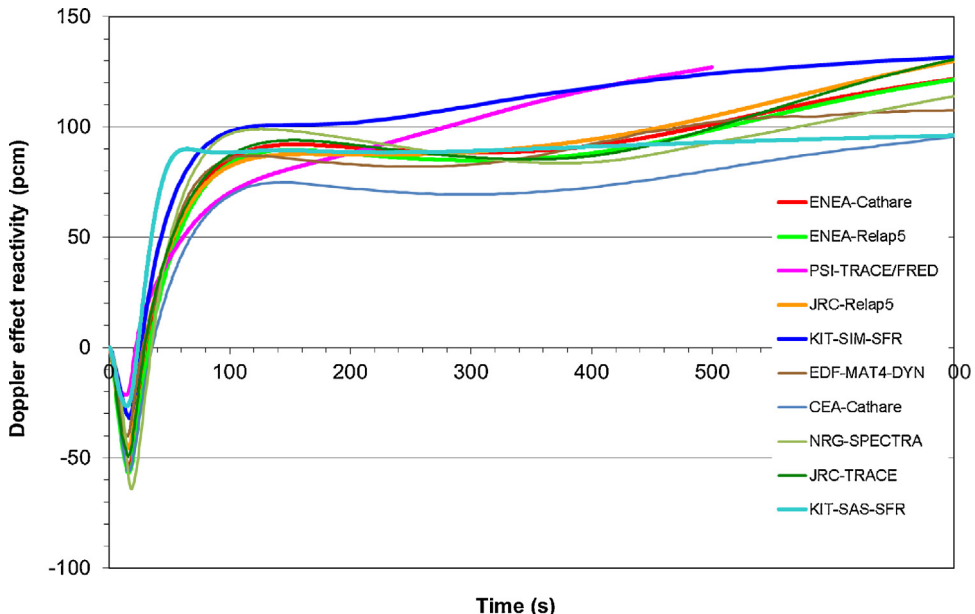


Fig. 13. Doppler effect reactivity.

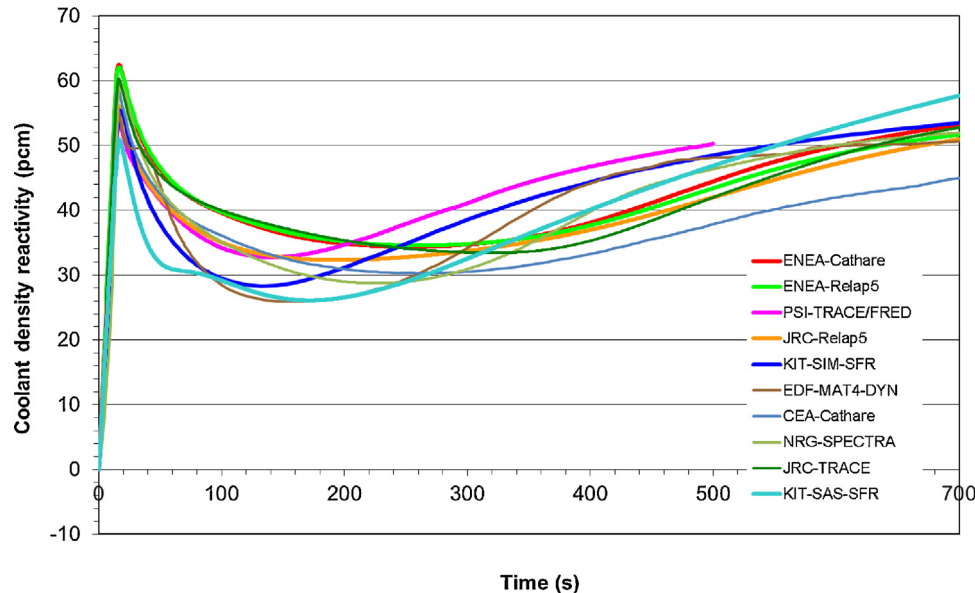


Fig. 14. Coolant density reactivity.

temperatures (see Fig. 9). After the maximum coolant temperature is reached all the codes predict a similar behaviour as the results are gathered in a relatively narrow band. The outlet temperature evolves to a new equilibrium state at a higher value for this particular transient. SAS-SFR shows a steeper increase of the temperature over time as the sodium temperature at the core outlet is evaluated by averaging the coolant temperatures at SA outlet of the individual fissile channels. This SAS-SFR averaging procedure may not be fully consistent with the way the transient variation of the coolant outlet temperature is defined in the calculation results presented by the other participants of the exercise.

The steam temperature at the steam generator outlet (Fig. 10) presents a much wider range of predicted values by the different partners' calculations. Even though they predict that the temperature stabilises at a value between 650 °C and 680 °C its evolution during the first seconds of the transient display notable differences. The reasons behind these deviations among the partners are

possibly ascribable to the different modelling of the sodium/water thermal interface of the SG and the differences in the assumed thermal inertia of the secondary systems due to uncertainties in the ESFR BOP design. The difference in modelling of the dynamics of the water interface in the SG (highly superheated steam conditions) could be another reason for the observed deviations.

5.2. Fuel and cladding temperatures

Figs. 11 and 12 show the evolution of the fuel and cladding peak temperatures. These temperatures are taken from the highest loaded node from the fuel and cladding models respectively of the hot fuel assembly (peak power pin).

Fig. 11 shows that the peak fuel temperature at steady state presents values ranging from 2420 °C to 2500 °C. This value is strongly influenced by the degree of detail in modelling the fuel rod mechanical behaviour. Some of the codes have models that evaluate

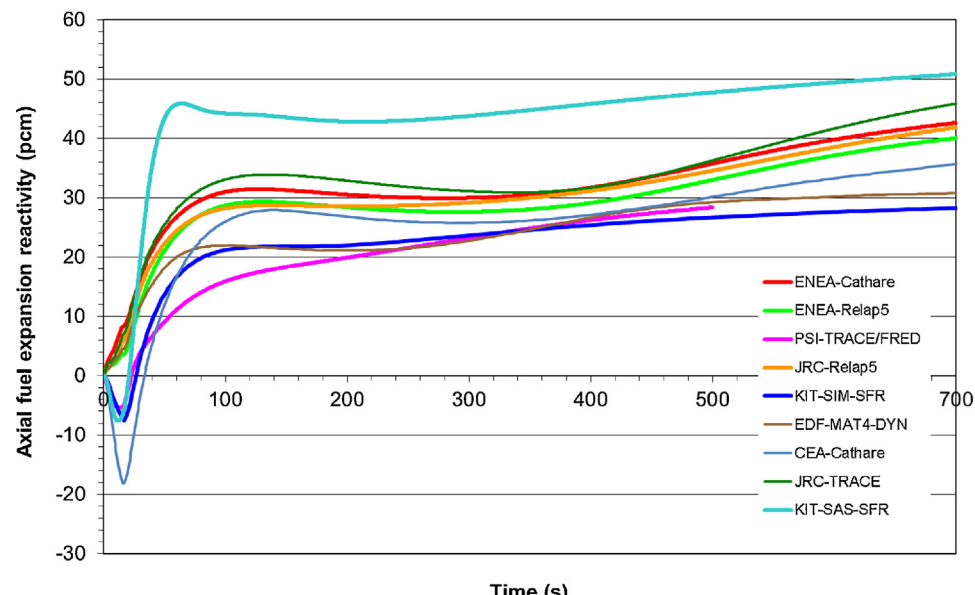


Fig. 15. Axial (fuel and cladding) expansion reactivity.

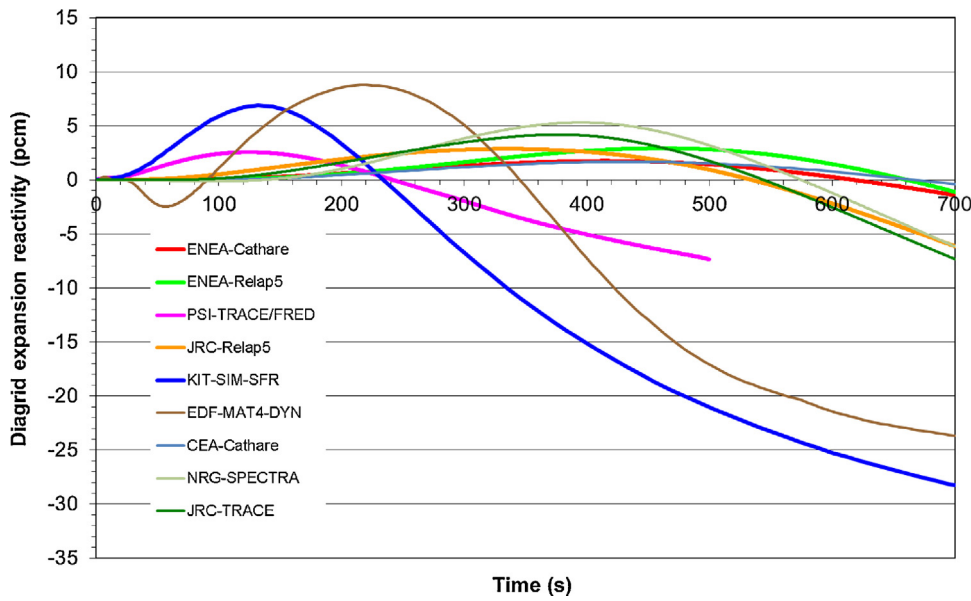


Fig. 16. Diagrid expansion reactivity.

the fuel-cladding gap dynamically. Other codes keep a constant gap size that underestimates fuel temperatures. A sensitivity analysis was performed between equivalent models developed by ENEA for CATHARE (dynamic model) and for RELAP5 (static model) showing that the difference is however limited for this particular transient (limited ULOF).SAS-SFR uses its built-in fuel behaviour simulation model DEFORM IV-C leading to smaller maximum initial fuel centre temperatures than the other codes. This temperature is strongly influenced by the development of the fuel-cladding gap size and the calculation of the heat conductivity along the gap. The gap size itself depends on the changes of the fuel and cladding during pre-irradiation by thermal expansion, swelling, and cracking. A detailed comparative analysis of all these effects is recommended in the future to isolate which physical effect is responsible for the deviation from the other codes. Additionally, SAS-SFR uses the average power of the highest loaded SA to define the peak power pin, not the individual pin. This leads to about 8–10%

less power and therefore to lower temperatures in the considered SA.

[Fig. 12](#) shows the evolution of the peak cladding temperature. It displays a maximum value in the range between 740 °C and 860 °C. This value is influenced by the massflow distribution in the different flow channels modelled differently by the different partners since the gagging specification is not clearly stated in the project documentation. This accounts for the relatively large band in calculated maximum clad temperatures. The cladding temperatures stabilise between 700 °C and 760 °C.

5.3. Reactivity feedback

[Fig. 13](#) shows the evolution of the Doppler reactivity feedback effect calculated by the different partners. It is related with the fuel temperature evolution as shown in [Fig. 11](#). During the first seconds

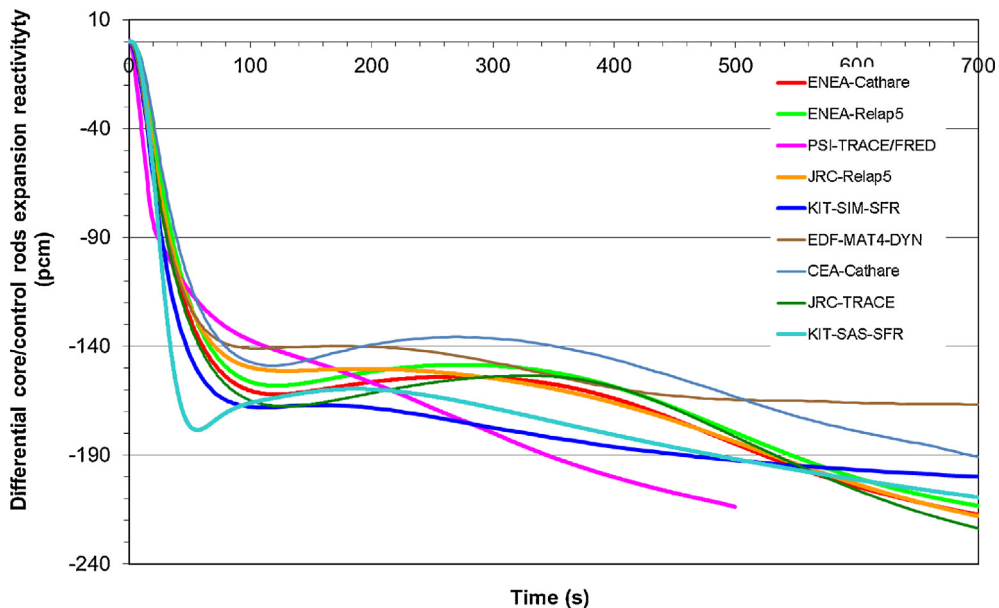


Fig. 17. Differential core/control rods expansion reactivity.

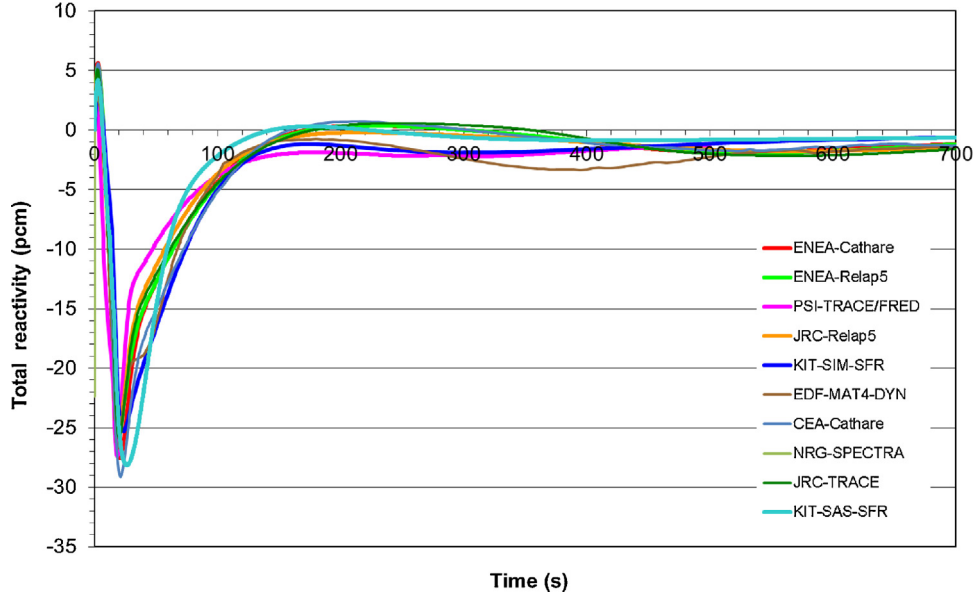


Fig. 18. Total reactivity.

of the transient the fuel temperature increases abruptly, this creates a negative reactivity that contributes to lower the reactor power.

Fig. 14 shows the evolution of the coolant expansion reactivity feedback. As this reactivity feedback is governed by a positive reactivity feedback coefficient the increase in the coolant temperature creates a positive reactivity contribution which has to be limited by design measures in order to prevent this reactivity component to become excessively positive (as may occur when the centre of the core should become voided). This effect must then be counterbalanced by other negative reactivity feedbacks in order to prevent power excursions. In this particular transient (flow-coast down to 40%), core voiding was not reached as the coolant outlet temperatures remained significantly below ($\sim 200^\circ\text{C}$) the boiling point of the sodium coolant ($\sim 935^\circ\text{C}$) as can be seen in Fig. 8.

Fig. 15 shows the evolution of the axial expansion reactivity effect. This effect is the combination of the fuel axial expansion

effect Eq. (3) and the cladding expansion effect Eq. (4). As is related with the fuel temperature, as stated in Eq. (3), it has a similar reactivity response as the Doppler effect but is of lower value. So, it also contributes to decrease the reactor power when the fuel becomes overheated. The effects of the particular model in SAS-SFR are clearly visible.

Fig. 16 shows the effect of the radial expansion of the diagrid due to thermal effects. There is a significant deviation between the different partner's results. The main cause of this spread is the uncertainty about the thermal inertia of the diagrid structure and the evolution of the outlet temperature of the intermediate heat exchanger, as reflected in the evolution of the core inlet temperature (Fig. 9), which leads consequently to correspondingly different reactivity feedback responses. It should be noted that this reactivity component is smaller than most of the other reactivity components, so its contribution to the total reactivity evolution is rather

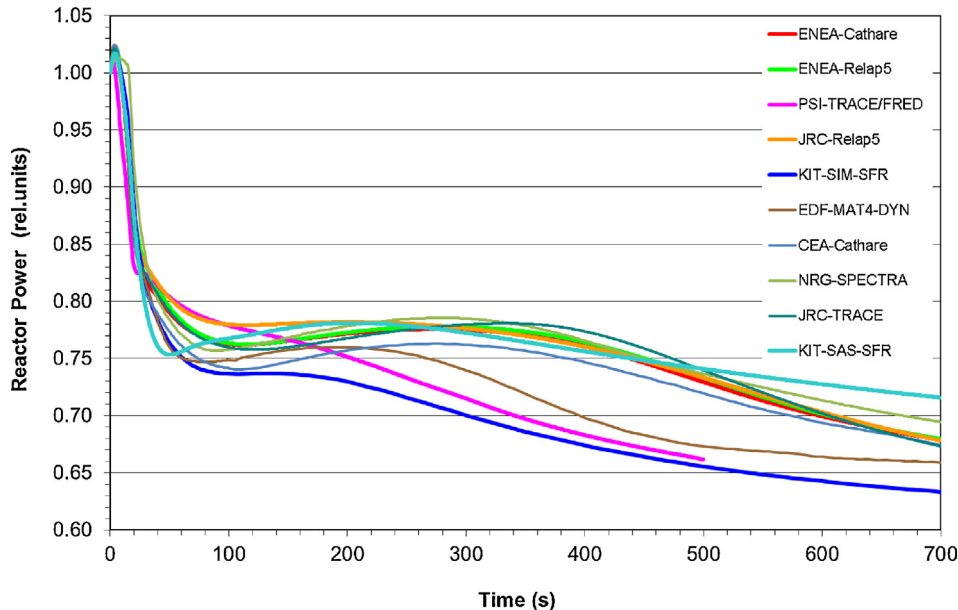


Fig. 19. Reactor power.

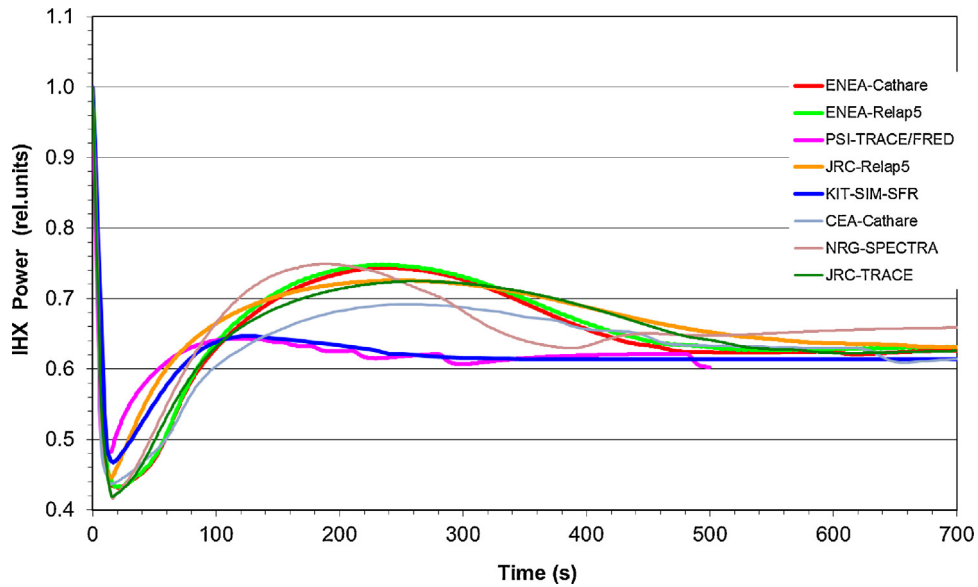


Fig. 20. IHX power.

limited. Besides, models for this feedback coefficient have not yet been validated by corresponding operational plant data.

Fig. 17 represents the reactivity feedback evolution caused by the partial insertion of the control rods due to the differential core/control rod thermal expansion. As it can be observed by the reactivity feedback scale it is a very strong negative reactivity feedback component causing the reactor power to decrease substantially during this transient. This effect is the most important feedback component in ESFR under BOL conditions assuring the reduction of reactor power in the case of the overheating of the core coolant and structures. The deviations among the partners' calculations, though limited, are caused by the combined influence of the differences of core inlet, core outlet and upper plenum coolant temperatures.

Fig. 18 shows the total reactivity feedback evolution of this transient. It is composed of the various contributions of the above mentioned individual reactivity feedback effects. It is important to highlight that during the first seconds of this particular transient

the reactor power increases slightly (initially to $\sim 103\%$ nominal value) due to the positive reactivity created by the coolant expansion effect. This effect is then counterbalanced by the various other reactivity feedback components such as the Doppler effect, and in particular the thermal expansion of the control rods effectively decreasing reactor power thereafter.

There is a satisfactory level of agreement between the different partners' calculational results to this "limited" ULOF event (40% primary flow reduction). This agreement is of particular importance as the total reactivity determines the reactor power behaviour, which in turn is of importance for the safety assessment of the entire system.

5.4. Powers

The total reactivity feedback leads to the power evolution as shown in Fig. 19. During the earlier seconds of the transient the reactor slightly increases in power. Thereafter, the negative

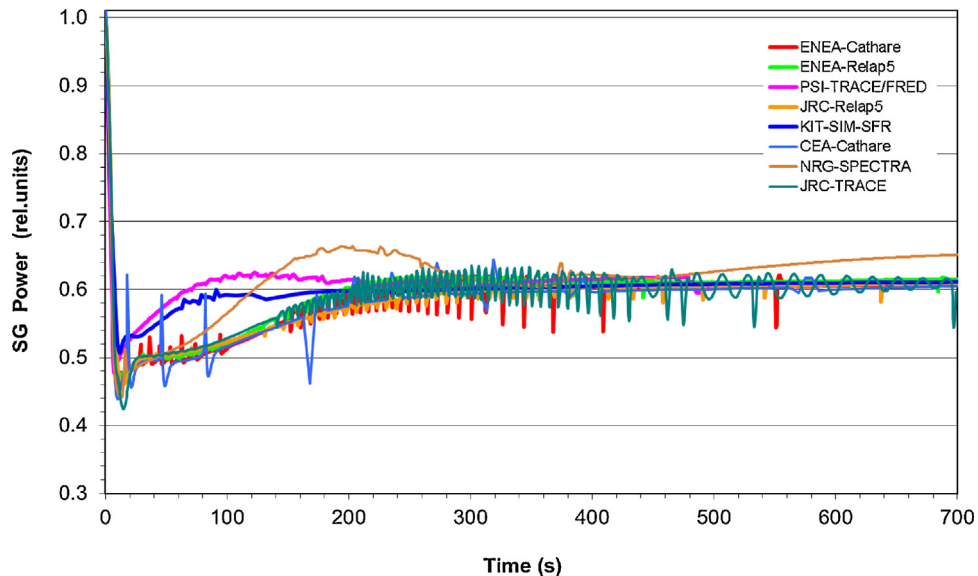


Fig. 21. SG power.

reactivity created by the Doppler effect and the differential core/control rod expansion effect reduces the reactor power. The different partners calculated the peak power at around 103% nominal, with a power reduction to 70% to 63% during the time interval considered (700 s).

The evolution of the powers exchanged in the IHXs and SGs are shown in Figs. 20 and 21. Due to the reduction of the sodium mass flow on the primary side the power exchanged from the primary to secondary and tertiary systems is significantly reduced. After the initial power undershoot to below 50% in the IHX (see Fig. 20) and below 55% in the SG (see Fig. 21) the power increases again as the primary coolant temperature increases. The observed deviations between the participants in these figures are caused by the different modelling assumptions of the secondary loops (uncertainty about coolant inventory). The asymptotic value of ~60% of nominal power is predicted quite consistently by all codes.

The heat exchanged in the SGs between the secondary and tertiary circuits follows the trend imposed by the power exchanged between the primary and secondary circuits in the IHX. It is also influenced by the different secondary inventory assumed by the different partners. The final value after 700 seconds transient time is again quite close to ~60% nominal value.

6. Conclusions

With the objective of harmonization of computational tools to assess the safety performance of new reactor concepts a dedicated task was established within the framework of the CP-ESFR project.

In this paper the results of a comparison benchmark case (unprotected loss of flow type) are presented using different codes (CATHARE, MAT4-DYN, RELAP, TRACE, SIM-SFR, SAS-SFR, SPECTRA, etc.) as developed or adapted by different organizations (CEA, EDF, ENEA, PSI, KIT, JRC, NRG). The goal was to assure consistency in the applied methodology and modelling of the codes, as well as in the specification of the plant main design parameters.

In general terms the benchmark demonstrated good agreement among the various codes in the various parameters calculated that are relevant for safety, considering the complexity of the different codes, their different origin, and quite different modelling approaches. The participants of the benchmark comparison case have quite consistently calculated the main parameters of the transient and have thus demonstrated to be able to simulate the transient behaviour of SFR reactors under turbulent, forced flow conditions.

The main outcome of this study is that all codes used are able to analyse the transient behaviour of the ESFR plant design. In some cases, appropriate code specific modifications were made. In the benchmark case the code results were compared and the following deficiencies were identified:

- Even though its effect was limited in this transient, the use of static or dynamic fuel-cladding gap size model affects the calculation of the fuel temperature and thus the associated reactivity feedback effects (i.e., Doppler, axial expansion). So, its implementation is advisable for transient analysis where higher fuel temperature variations under different core states (specifically BOL, EOL) are observed.
- There is uncertainty about the time delay constant associated with the heat-up of the diagrid plate and the corresponding evolution of the core radial expansion reactivity feedback effect.
- There is uncertainty in the geometrical definition of the secondary systems that lead to different secondary circuit thermal inertias and consequently to differences in the transient temperatures of the primary/secondary/tertiary system configuration.

- There is need to harmonize methodologies to calculate mean values, such as fuel mean temperatures, that may affect some safety parameters such as the Doppler and axial fuel expansion reactivity feedback effects.

It is important to underline the great effort made by all participants to properly account for the uncertainties and the simulation challenges, the fruitful discussions helping in narrowing down the differences in their calculated results, and to close gaps in available plant design data base.

The benchmark was consequently a good basis from which to undertake the full set of calculations for representative transients. This analysis will be the subject of the second part of the article.

Acknowledgements

We would like to acknowledge the financial support given to the project by the European Commission through the Seventh Framework Programme (FP7).

References

- Blanchet, D., Buiron, L., 2009. ESFR Working horse description. In: European Sodium Fast Reactor Reactor Consortium, Deliverable SP2.1.2.D1.
- Becker, M., Van Criekingen, S., Broeders, C.H.M., 2010. The KARlsruhe PROgram System KAPROS and its successor the Karlsruhe Neutronic Extendable Tool KANEXT. <http://inrwww.webarchiv.kit.edu/kanext.html>
- Bubelis, E., Schikorr, M., 2012. Personal communication.
- Chenu, A., EPFL Thesis 5172 2011a. Single- and two-phase flow modelling for coupled neutronics/thermal-hydraulics transient analysis of advanced sodium-cooled fast reactors'. <http://dx.doi.org/10.5075/epfl-thesis-5172>.
- Chenu, A., 2011b. Pressure drop modeling and comparisons with experiments for single- and two-phase sodium flow. Nuclear Engineering and Design 241 (9), 3898–3909.
- Chetal, S.C., Balasubramanian, V., Chellapandi, P., Mohanakrishnan, P., Puthiyavinyagam, P., Pillai, C.P., Raghupathy, S., Shamugham, T.K., Sivathanu Pillai, C., 2006. Design of prototype fast Breeder reactor. Nuclear Engineering and Design 236 (7–8), 852–860.
- Darmet, G., Massara, S., 2012. Dynamical analysis of innovative core designs facing unprotected transients with the MAT5-DYN code. In: Proceedings of ICAPP 2012, paper 12245.
- Dufour, Ph., et al., 2011. Comparison Case. Deliverable SP3.3.1 D0.
- Ehster, S., 2009. Safety objectives and design principles. In: European Sodium Fast Reactor Reactor Consortium, Deliverable SP3.1 D1.
- European Utility Requirements for LWR Nuclear Power Plants, 2001. Revision C.
- ESNII, 2009. Strategic Research Agenda.
- Fiorini, G.L., 2013. CR ESFR—description of the work. In: CP-ESFR Documentation.
- Geffraye, G., et al., 2011. CATHARE 2 V2.5 2: A single version for various applications. Nuclear Engineering and Design 241, 4456–4463.
- Gen IV Roadmap, December 2002. US DOE Nuclear Energy Research Advisory Committee and the Generation IV International Forum, A Technology Roadmap for Generation IV Nuclear Energy Systems, GIF002-00.
- Genot, J.-S., 2009. ESFR working horse loop concept description. In: European Sodium Fast Reactor Reactor Consortium, Deliverable D4.1.1.
- Kondo, S., et al., 2013. Recent progress and status of Monju. In: Proceedings of the International Conference on Fast Reactors and Related Fuel Cycles (FR13) Paper CN-199-030.
- Lassmann, K., Hohlefeld, F., 1987. The revised URGAP-model to describe the gap conductance between fuel and cladding. Nuclear Engineering and Design 103, 215–221.
- Le Coz, P., 2013. The ASTRID project: status and future prospects. In: Proceedings of the International Conference on Fast Reactors and Related Fuel Cycles (FR13) Paper CN-199-261.
- Massara, S., et al., 2005. Dynamics of critical dedicated cores for minor actinide transmutation. Nuclear Technology 149, 150–174.
- Matsuura, M., et al., 2007. Design and modification of steam generator safety system of FBR MONJU. Nuclear Engineering and Design 237 (12–13), 1419–1428.
- Mikityuk, K., 2009. Heat transfer to liquid metal: review of data and correlations for tube bundles. Nuclear Engineering and Design 239, 680–687.
- Mikityuk, K., Krepel, J., 2010. Specification of the BOL O-ESFR core model for transient analysis. In: CP-ESFR Documentation.
- Mikityuk, K., Shestopalov, A., 2011. FRED fuel behaviour code: main models and analysis of Halden FA-503. 2 tests. Nuclear Engineering and Design 241, 2455–2461, DOI:10.1016/j.nucengdes.2011.04.033.
- NRC, 2007. TRACE v5.0 Theory and User's Manual. Office for Nuclear Regulatory Research, Washington.
- NRG, Version 3.60, Volume 1—Program Description, Volume 2—User's Guide, Volume 3—Subroutine Description, Volume 4—Verification and Validation, NRG

- Report K5024/10.101640. Arnhem 2010. M.M. Stempniewicz, SPECTRA Sophisticated Plant Evaluation Code for Thermal-hydraulic Response Assessment.
- Phillipponneau, Y., 1992. Thermal conductivity of $(u, Pu)O_2-x$ mixed oxide fuel. *Journal of Nuclear Materials* 188, 194–197.
- RELAP5/MOD3 Code Manual, 1995. Vol 2. NUREG/CR-5335-Vol II. Office for Nuclear Regulatory Research, Washington.
- Schikorr, W.M., 2001. Assessment of the kinetic and dynamic transient behaviour of sub-critical systems (ADS) in comparison to critical reactor systems". *Nuclear Engineering and Design* 210, 95–123.
- Sauvage, J.F., 2005. Phenix, Une histoire de coeur et d'energie. Commissariat à l'Energie Atomique.
- Saraev, O.M., Noskov, Yu.V., Zverev, D.L., Vasilev, B.A., Sedakov, V.Yu., Poplavskii, V.M., Tsibulya, A.M., Ershov, S.G., Znamenskii, V.N., 2012. BN-800 design validation and construction status". *Atomic Energy* 108 (4), 248–253.
- Vasile, A., et al., 2011. European Commission—7th Framework Programme "The Collaborative Project on European Sodium Fast Reactor (CP-ESFR)". *Nuclear Engineering and Design* 241, 3461–3469.
- Xu, M., 2000. Chinese fast reactor technology development. In: The 5th Nuclear Energy Symposium on Energy Future in the Asia/Pacific Region—Research & Education for Nuclear Energy, Beijing, pp. 28–37.